

Article

Activated Carbon-Spinels Composites for Waste Water Treatment

Ernesto de la Torre *, Ana Belén Lozada, Maricarmen Adatty and Sebastián Gámez 

Department of Extractive Metallurgy, Escuela Politécnica Nacional, Ladrón de Guevara E11-253, Quito 170517, Ecuador; anibelen_93@hotmail.es (A.B.L.); mary.a_3093@hotmail.com (M.A.); sebastian.gomez@epn.edu.ec (S.G.)

* Correspondence: ernesto.delatorre@epn.edu.ec; Tel.: +593-(9)9947-1051

Received: 29 November 2018; Accepted: 14 December 2018; Published: 16 December 2018



Abstract: Nowadays, mining effluents have several contaminants that produce great damage to the environment, cyanide chief among them. Ferrites synthesized from transition metals have oxidative properties that can be used for cyanide oxidation due to their low solubility. In this study, cobalt and copper ferrites were synthesized via the precipitation method, using cobalt nitrate, copper nitrate, and iron nitrate as precursors in a molar ratio of Co or Cu:Fe = 1:2 and NaOH as the precipitating agent. The synthesized ferrites were impregnated in specific areas on active carbon. These composites were characterized using X-Ray Diffraction (XRD) and Scanning Electron Spectroscopy (SEM). The XRD results revealed a cubic spinel structure of ferrites with a single phase of cobalt ferrite and two phases (copper ferrite and copper oxides) for copper. The CoFe_2O_4 impregnated on active carbon reached a cyanide oxidation of 98% after 8 h of agitation; the composite could be recycled five times with an 18% decrease in the catalytic activity. In cobalt ferrites, a greater dissolution of iron than cobalt was obtained. In the case of copper ferrite, however, the copper dissolution was higher. These results confirm that ferrites and activated carbon composites are a novel alternative for cyanide treatment in mining effluents.

Keywords: copper ferrite; cobalt ferrite; activated carbon; cyanide oxidation

1. Introduction

The effluents generated during metallurgical operations, galvanizing, gold and silver extraction, crude refining, among others, contain metal complexes of cyanide or free cyanide [1]. The Environmental Protection Agency (EPA) catalogs this waste as highly dangerous for nature and human health, thus its treatment prior to discharge in water bodies is a very important issue [2]. Therefore, several methods have been applied through the years in order to oxidize cyanide to cyanate ions. The cost of cyanide oxidation with hydrogen peroxide or expensive acid reaches 4 USD/kg CN^- , so it is necessary to look for other alternatives that allow for the treatment of cyanide without spending expensive reagents [3].

In the last few years, several composites based in biomass or active carbon have been employed for waste water treatment. The importance of these composites lies in their easy separation of products or reagents without operations such as filtration, centrifugation, or decantation. In case of losing its activity, these composites can be reactivated using thermal processes. The latest advances that are focused on green chemistry, development of clean technologies, and sustainability point to a heterogeneous catalysis as the solution for these challenges. In the particular case of cyanide ions oxidation coming from metallurgical operations, activated carbon may transform this toxic reagent into more environmentally friendly substances. In addition, activated carbon may be used as an ideal support in order to develop catalysts that can be used as oxidizing agents [4,5].

Ferrites formed from transition metals are widely studied, due to their use as magnetic materials, semiconductors, pigments, and catalysts. These are classified according to their crystallization structure: hexagonal ($MFe_{12}O_{19}$), garnet ($M_3Fe_5O_{12}$), and spinel (MFe_2O_4), where M is one or more divalent transition metals (Mn, Fe, Co, Ni, Cu, and Zn) [6]. The catalytic properties of the different ferrites are given by the transition metals present in the structure and the distribution of the same. Thus, ferrites are used in alkylation processes, phenol hydroxylation, hydrodesulfurization of crude, and oxidation of various compounds, among others. In addition, their advantage lies in the fact that its magnetic properties facilitate its recovery through the use of a magnet [7].

Copper and cobalt ferrites generally have a spinel structure with a mixed distribution, where Cu^{2+} and Co^{2+} ions are distributed in both the tetrahedral (A) and octahedral (B) positions. This distribution is influenced by the temperature; at room temperature, the Cu^{2+} or Co^{2+} ions occupy the positions B, while the Fe^{3+} ions are located evenly in the positions A and B, that is to say a spinel of inverse structure. At temperatures above 360 °C, the Cu^{2+} or Co^{2+} ions occupy positions A, and the spinel has a normal structure that improves the magnetic properties of the ferrite [8].

Conventional methods of copper and cobalt ferrite synthesis, such as chemical precipitation or the sol-gel method, give rise to a ferrite with a reverse spinel structure. In addition, from these methods it is not possible to obtain a stoichiometric copper or cobalt ferrite since there will always be the presence of a second phase formed by CuO or CoO. In the case of copper ferrites, the maximum copper concentration in a Copper Ferrite is given by the following formula, $Cu_{1-n}Fe_{2+n}O_4$, where $n = 0.04 \pm 0.01$ [9,10].

The high catalytic activity of ferrites is related to the weak bond between oxygen and the metal with the highest oxidation state [11]. Then, the catalyst may follow the Mars van Krevelen mechanism in order to oxidize cyanide ions into cyanates [12]. The Mars-van Krevelen mechanism is a redox cycle in which the reagent interacts with the catalyst in an active site that contains an M_1 metal cation, adsorbed on the surface. The oxygen in the catalyst migrates to the surface to oxidize the adsorbed reagent (cyanide ions in this case) and form the products. Spent oxygen is rapidly replaced either by oxygen from the gas phase or by oxygen associated with another M_2 cation [13,14].

Table 1 shows the results of previous studies for the oxidation of cyanide ion using cobalt and nickel ferrites, as well as cobalt and manganese oxide systems. The cobalt oxides are not very efficient for the oxidation of the cyanide ion. However, the addition of another transition metal such as manganese, which has high catalytic activity, doubled the oxidation percentage [2]. If instead of a cobalt oxide, a cobalt ferrite or a nickel ferrite is used, the percentage of oxidation is 85%, which shows that the catalytic activity of the cobalt ferrite is superior to that of the oxide systems.

Table 1. Cyanide oxidation results with different oxide systems.

Composite	Cyanide Ion Oxidation (%)	References
CoO	41%	S. Christoskova and Stoyanova, 2009 [2]
CoO-MnO	83%	
CoFe ₂ O ₄	85%	Stoyanova, Christoskova and Georgieva, 2004 [15]
NiFe ₂ O ₄	85%	M. K. Stoyanova and Christoskova, 2005 [16]

Moreover, unlike other catalysts, such as oxide systems, copper and cobalt ferrites have refractory characteristics, which imply that copper and cobalt dissolution in cyanide solutions is very low, approximately 4% for Cu or Co and 1% for Fe after 15 h [17].

Nowadays, several waste water treatment processes have been implemented in order to remove various contaminants. For instance, Alexopoulou and co-workers [18] employed copper (I) phosphide along with sodium persulfate for the degradation of sulfamethoxazole using the formation of radicals. Other contaminants, such as ibuprofen found in multiple water bodies, may be degraded by hydrodynamic cavitation [19]. This degradation was carried out in a Venturi reactor and caused a cavitation where 60% of ibuprofen was degraded in 60 min [19]. Ultrasonic methods along with ozone,

hydrogen peroxide, and Fenton have recently been assessed for waste water treatment. In this study, the combination of Fenton with ultrasonic flow cell delivered the best chemical oxygen demand (COD) removal [20].

Other materials oriented for water treatment are metal organic frameworks (MOFs) for heavy metals removal. Fe (III) and Zr (IV) based metal–organic frameworks supported on polyacrylonitrile (PAN) and polyvinylidene fluoride (PVDF) nanofibers were successfully employed for lead and mercury removal from solutions. This supported material allowed to treat 395 mL of 100 ppb Pb (II) solution in order to reduce its concentration to 10 ppb, which is the limit permitted for drinking water [21]. Other variety of MOFs supported on nanofibers presented excellent results in the removal of cadmium and zinc ions from aqueous solutions. These (Zr-based MOF-808) supported on PAN nanofibers allowed treat a reasonable amount of Cd solution at a flux of 348 L m²/h [22]. These kinds of materials can be used in a filtration operation for heavy metal adsorption-desorption experiments. In addition, permeate behavior of supported MOFs can be predicted accurately in order to know MOFs adsorption capacity [23].

The present work is oriented to the synthesis of a catalyst based on oxides of iron, copper, and cobalt that accelerates the oxidation of the cyanide ion present in the effluents coming from the extraction of gold, prior to its discharge in the hydric bodies due to its high toxicity. The advantage of this work is that the cobalt and copper ferrites composites can be used in effluents with high concentrations of cyanide since they do not generate toxic residues. Due to the availability of copper, cyanide ions oxidation with these kind of ferrites makes this treatment less expensive than other conventional methods. For instance, electrochemical oxidation that demands a high energy consumption [2] and of chemical oxidation with hydrogen peroxide or peroxosulfuric acid where the reagents used are very expensive [3].

2. Materials and Methods

2.1. Materials

Copper ferrite and cobalt ferrite were prepared by a precipitation method. Iron nitrate Fe(NO₃)₃·9H₂O (Merck, 98%), copper nitrate Cu(NO₃)₂·3H₂O (Sigma Aldrich, 99%), and cobalt nitrate Co(NO₃)₂·6H₂O (Sigma Aldrich, 99%) were used as precursor salts. Sulfuric acid (H₂SO₄) (Mallinckrodt, 98%) was used in order to wash the composites. Nitric acid (HNO₃) and hydrofluoric acid (HF) (Merck, 68%), were employed in acid disintegration tests. Silver nitrate (AgNO₃) reactive grade (Scharlau) was employed for free cyanide quantification by titration. Sodium cyanide (NaCN) and sodium hydroxide (NaOH) of a technical grade were employed for oxidation essays.

2.2. Synthesis of Copper Ferrite

For the synthesis of copper ferrite (CuFe), a solution of Cu(NO₃)₂·3H₂O and Fe(NO₃)₃·9H₂O reactive grade was used with a Cu:Fe molar ratio of 1:2 [24]. Then, a 1.0 M NaOH solution was added until the mixture reached a pH value of 6 with constant magnetic stirring for 2 h [9]. The precipitate was then filtered and washed with distilled water. Afterwards, the precipitate was dried at 110 °C for 16 h and then calcined for 4 h at 750 °C. Finally, an acid wash was carried out with 2% v/v sulfuric acid to eliminate the soluble copper oxides.

2.3. Synthesis of Cobalt Ferrite

A 0.5 M solution of cobalt nitrate and iron nitrate was prepared with a molar ratio Co:Fe = 0.5, and a 0.4 M solution of sodium hydroxide. The nitrate solution was placed in a vessel and subjected to constant magnetic stirring, while the precipitating agent, sodium hydroxide, was added until the mixture and reached a pH value equal to 7. The stirring was carried out at room temperature for 2 h. Then, the precipitate was filtered and washed with distilled water. Afterwards, the precipitate was dried at 110 °C for 16 h and finally calcined at 750 °C for 4 h. In order to eliminate the possible cobalt

and iron oxides present in the obtained product, an acid wash was carried out with a 2% v/v sulfuric acid solution until a transparent solution was obtained as a product of the filtration.

2.4. Activated Carbon-Spinles Composites Preparation

The activated carbon-spinels composites were prepared by adding activated carbon of 280 m²/g (AC280) and 1000 m²/g (AC1000) of specific surface in the copper-iron and cobalt-iron solutions. The mass ratio between ferrite and activated carbon was 1:1 and a 5.0 M sodium hydroxide solution was added in order to achieve a pH = 12 under continuous stirring for 1 h. Then the obtained composites were dried overnight at 110 °C and employed for oxidation essays. An additional calcination stage was implemented as well, which consisted of heating for 2 h at 700 °C in a crucible with a lid, in order to prevent the combustion of carbon. Finally, the acid wash was carried out with a sulfuric acid solution 2% v/v in order to eliminate all copper and cobalt oxides.

2.5. Characterization

Ferrites and activated carbon composites were characterized using an X-ray diffractometer (XRD) Bruker AXS D8 Advance model (Bruker, Karlsruhe, Germany) and a scanning electron microscopy (SEM)-electric dispersive scanning (EDS) Vega TESCAN (TESCAN, Brno, Czech Republic), as well as a BET surface area with a Quantachrome Instruments Nova4200e (Quantachrome Instruments, Boynton Beach, FL, USA). In order to determine the impregnation of copper and cobalt ferrites on activated carbon, all composites were disintegrated with 6 mL of HNO₃ and 2 mL of HF. Copper and cobalt in the solutions were analyzed by atomic absorption spectroscopy with a Perkin Elmer AAnalyst 300 spectrometer (Perkin Elmer, Shelton, CT, USA). The impregnation percentage of copper and cobalt ferrites on activated carbon was determined from the following equation:

$$\% \text{Impregnation} = \frac{\text{Copper or cobalt ferrite mass}}{\text{Active carbon mass}} \times 100\% \quad (1)$$

2.6. Catalytic Oxidation Procedure

Catalytic activity of the ferrites and activated carbon composites was measured during all oxidation essays. The oxidation was carried out in a 500 mL volume reactor with continuous mechanical stirring of 480 rpm and air inlet of 180 NL/h at room temperature (20 °C). A 500 mg/L solution of NaCN was prepared, the pH was adjusted throughout the oxidation procedure to a value above 10.5, with the addition of NaOH. The ratio between the material and the cyanide concentration was maintained at 15 g composite/g CN⁻/L. Samples of 5 mL were taken each hour to analyze the residual cyanide by titration with a 4.33 g/L AgNO₃ solution. In addition, a set of 10 mL samples were taken each hour for 8 h in order to measure the dissolution of copper and cobalt in the cyanide solution by atomic absorption spectroscopy. The cyanide ion oxidation was determined with the following equation:

$$\% \text{Oxidation} = \frac{[\text{CN}^-]_{t=0} - [\text{CN}^-]_t}{[\text{CN}^-]_{t=0}} \times 100\% \quad (2)$$

The catalysts samples were named CuFe and CoFe for bulk copper and cobalt ferrites, respectively. CuFe-AC280, CuFe-AC1000, CoFe-AC280, and CoFe-AC1000 for supported catalysts with activated carbon of 280 m²/g and 1000 m²/g of specific surface, respectively.

3. Results and Discussion

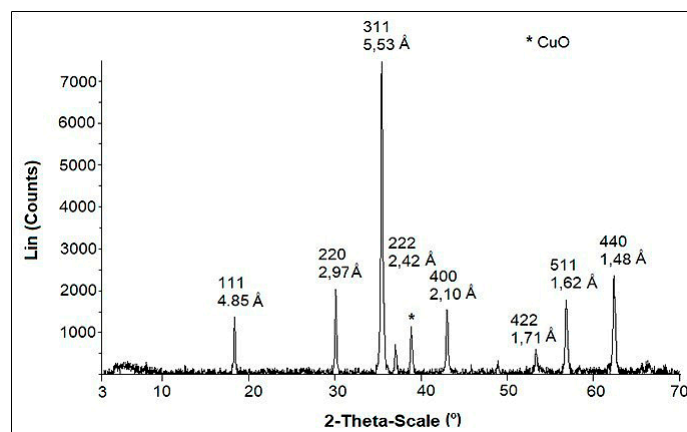
As it was mentioned in the Materials and Methods section, two activated carbons of different specific area were employed as supports for ferrites deposition. In Table 2, it is summarized the main characteristics of the supports before and after impregnation.

Table 2. Composites characteristics before and after impregnation.

Composite	Specific Surface (m ² /g)	Bulk Density (g/cm ³)	Pore Size (Å)
AC280	280 ± 42	1.30 ± 2	7.37 ± 4
AC1000	1000 ± 58	1.30 ± 5	1.83 ± 2
CuFe-AC280	236 ± 15	1.35 ± 2	7.37 ± 5
CoFe-AC280	232 ± 18	1.36 ± 1	7.37 ± 2
CuFe-AC1000	906 ± 22	1.52 ± 1	1.83 ± 3
CoFe-AC1000	905 ± 36	1.50 ± 3	1.83 ± 2

In the case of specific surface, it is appreciable that ferrites deposition diminished activated carbons available area. Nevertheless, this specific surface reduction was not high; therefore, it can be inferred that ferrite deposited on activated carbon surface instead of within their pores. This assumption was confirmed when the composite pore size was analyzed. This parameter was not affected at all after ferrites impregnation essays. Finally, composites bulk density increased in all cases when copper and cobalt ferrites were deposited on activated carbon surface. This phenomenon was expected since ferrite deposition increased the composites mass.

The X-ray Diffraction analysis presented in Figure 1 showed the presence of copper ferrite in the CuFe sample. As mentioned in the introduction, due to the precipitation method used for the synthesis of the catalysts, ferrite stoichiometry was not obtained. In the composite, three phases were formed, which correspond to copper oxide (CuO), magnetite (Fe₃O₄) in smaller quantities, and the copper ferrite (CuFe₂O₄) in its majority. The peaks 220, 311, 400, 511, and 440 shown in the diffractogram are typical of a cubic copper ferrite, while the remaining peaks correspond to the copper oxide and magnetite. This was corroborated with the analysis using the atomic absorption spectroscopy with which a Fe:Cu molar ratio equal to 2.3 was determined. The excess of iron present in the sample was the result of the conditions and the method of synthesis as well as the acid wash, where the soluble copper oxide was removed. In addition, with these data we can infer that the copper ferrite adopted a reverse spinel structure.

**Figure 1.** X-ray Diffraction (XRD) patterns of copper ferrite synthesized using the precipitation method.

In the case of cobalt ferrite, the corresponding diffractogram is shown in Figure 2. The presence of (1 1 1), (2 2 0), (3 1 1), (2 2 2), (4 0 0), (5 1 1), (4 0 0) show the formation mainly of the spinel cubes of cobalt ferrite. There are less pronounced peaks that correspond to iron oxides in the form of magnetite Fe₃O₄ and maghemite γ -Fe₂O₃, which are also spinels. In contrast with copper ferrite synthesis, there was no cobalt oxides peaks in the diffractogram.

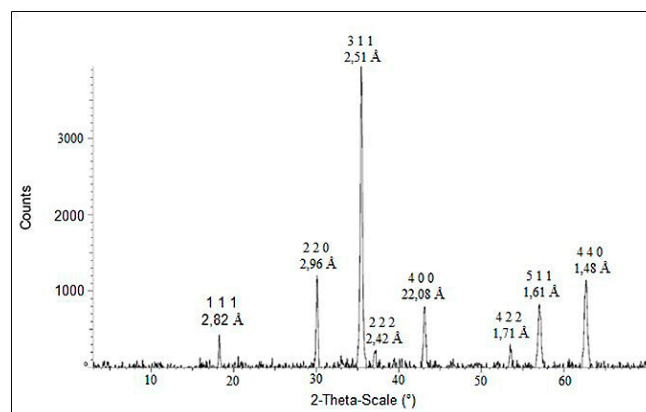


Figure 2. XRD patterns of cobalt ferrite synthesized using the precipitation method.

The results obtained using atomic absorption spectroscopy for the copper ferrite supported on activated carbon were similar to those obtained with the unsupported catalyst. This similarity lies in a greater presence of iron than copper as shown in Table 3. As regard with the percentages of impregnation, it can be observed that for the CuFe-AC280 and CuFe-AC1000 samples that were not calcined before the acid wash, the percentage of impregnation are 0.32% and 0.26%, respectively. This may be due to the fact that AC1000, which is a carbon of higher activation, is microporous, which makes it difficult for the impregnation of copper ferrites. However, when the CuFe-AC1000 sample is calcined, the impregnation percentage rises to 4.32%. This high percentage may be the result of ferrite sintering on the carbon surface.

Table 3. Molar ratio and impregnation percentage for support catalysts.

Composite	Fe/Cu	Impregnation (%)	Composite	Fe/Co	Impregnation (%)
CuFe-AC280	2.4	0.32	CoFe-AC280	0.52	0.24
CuFe-AC1000 (without calcination)	2.5	0.26	CoFe-AC1000 (without calcination)	0.52	0.28
CuFe-AC1000 (with calcination)	2.1	4.32	CoFe-AC1000 (with calcination)	0.53	7.47

In the case of cobalt ferrites on activated carbon, the impregnation of the cobalt ferrite within the carbon structure is significantly improved when the composite was calcined as well. The results indicate that the calcination temperature contributes to the formation of the respective cobalt and iron oxides after precipitating as hydroxides and allows the formation of the spinel structure. In addition, calcination performed in closed crucibles avoids damages in the structure of the support. With calcination, spinels formation is possible and their impregnation on active carbon was improved. The low percentages of impregnation obtained in the samples CuFe-AC280, CoFe-AC280, CuFe-AC1000, and CoFe-AC1000 without calcination can be due to the fact that the impregnation of the ferrite is superficial. Thus, cobalt and copper ferrites may be detached after a washing with sulfuric acid. These results agree with those reported by M.K. Stoyanova and Christoskova [16]. They reported that the calcination step was crucial for Ni-Fe oxides system formation and their performance in cyanide ion oxidation. Calcination may as well increase the amount of surface active oxygen and Fe³⁺ ions in high spin state. Therefore, calcination stage may improve the reducibility of Ni-Fe-oxide active oxygen [16].

Figure 3 shows the images obtained using scanning electron microscopy (SEM) of copper ferrites on activated carbon after calcination. It can be seen that the copper ferrite is not uniformly distributed on the surface of carbon since it tends to agglomerate at random sites on the surface, which may be the result of the ferrites sintering.

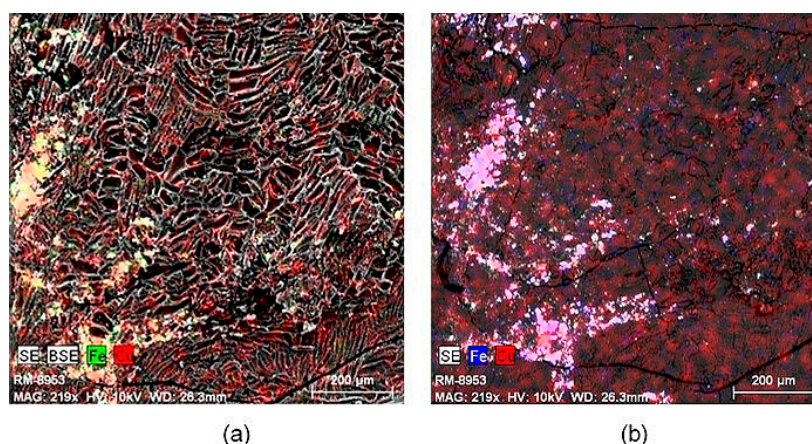


Figure 3. Scanning electron microscopy (SEM) images of $\text{CuFe}_2\text{O}_4/\text{AC1000}$ composite calcined: (a) by secondary electrons detector (SE); and (b) by backscattered electrons detector (BSE) a 219x.

Moreover, fractures can be distinguished on the surface of carbon, these are the result of constant agitation during impregnation as well as acid washing and also during calcination. All these operations weaken the support, which can lead to the loss of carbon during the oxidation tests, as well as the reduction of the life time of the composites.

In addition, the presence of agglomerates supports the idea of the polycrystalline structure, which is characteristic of spinels. However, it is clear that in this composite that the degree of crystallinity is low and there is a greater degree of typical defects of particles with super magnetic behavior (spinel). Figure S1 shows the morphological images of CoFe.AC1000 composite calcined (a) before the acid wash and (b) after the acid wash. Within cobalt and iron distribution, it can be observed that there are more depositions on the surface of active carbon before the acid wash than after the acid wash. This is due to the presence of the precipitating agent and cobalt oxides on the active surface. After the acid wash, cobalt and iron distribution is more uniform. A violet solution was obtained as washing solution that is characteristic of cobalt, so it confirms the elimination of cobalt oxide with the acid wash.

Cyanide oxidation experiments were carried out using eight different catalysts (CuFe , CoFe , AC280 , AC1000 , CuFe-AC280 , CuFe-AC1000 , CoFe-AC280 , and CoFe-AC1000) while maintaining an air flow of 180 NL/h, continuous mechanical stirring of 480 rpm, $\text{pH} = 10.5$ at 293 K. A decrease in cyanide concentration was determined by titration with a 4.33 g/L AgNO_3 solution; the results are reported in Figure 4.

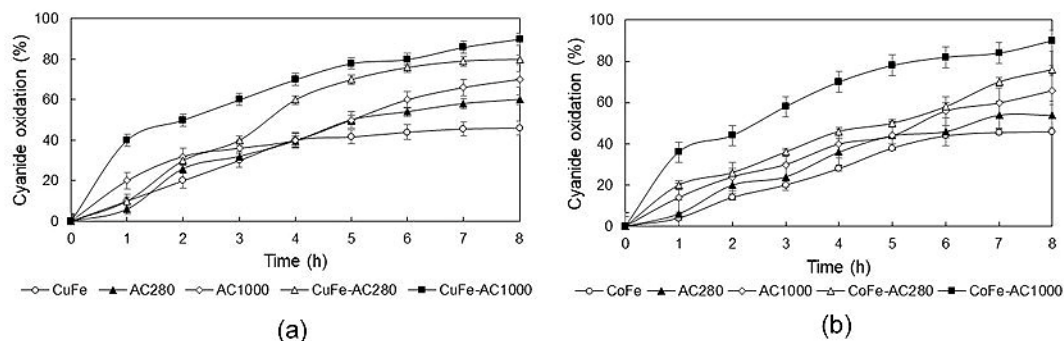
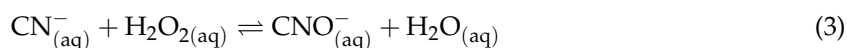


Figure 4. Cyanide oxidation with (a) copper ferrites-activated carbon composites and (b) cobalt ferrites-activated carbon composites. (Air flow = 180 NL/h; composite: solution ratio = 15 g/L.)

During preliminary tests, with an air flow of 180 NL/h, it was verified that cyanide oxidation was insignificant, reaching only a 10% after 8 h. When activated carbon was added to AC1000 or AC280 , the percentage of cyanide ion oxidation reached values of 70% and 60%, respectively, as

shown in Figure 4a. By replacing the activated carbon with the previously synthesized copper ferrite, an oxidation percentage of 46% was reached. The difference between the oxidation percentages reached is due to the reaction mechanism of each catalyst. Active carbon adsorbs molecular oxygen (O₂) provided with air on its surface, which reacts with the functional groups of the surface of the same forming hydrogen peroxide (H₂O₂). This reacts with the CN⁻ ion present in the solution as follows [25].



It is important to emphasize that, although active carbon adsorbs cyanide and this could contribute to the cyanide ion removal, according to the tests carried out by Pilco [26], the percentage of cyanide ion adsorption is less than 5%.

Cyanide oxidation is possible as well with the employment of cobalt ferrites on activated carbon, as can be observed in Figure 4b. Within the CoFe-AC280 composite, 76% of cyanide oxidation was achieved, whereas a 90% of cyanide oxidation was reached with the composite CoFe-AC1000. In the case of copper and cobalt ferrites, cyanide is oxidized via Mars van Krevelen mechanism. In this mechanism, an oxygen of the spinel structure reacts with cyanide ions and they are transformed into cyanates. In addition, the insertion of iron ions within the structure of the spinel is oriented to the generation of active sites on the characteristic structure of this composite.

Our results are similar to those obtained by Christoskova and Stoyanova [2]. They reported a 60% of cyanide ion oxidation after 2 h of agitation with manganese cobalt oxides at a pH of 12. In addition, they found that cyanide ion oxidation is better at a pH of 9.5. However, those results may be wrong, since cyanide may transform into hydrocyanic acid pH values lower than 10.5, which is a very toxic and volatile compound. Therefore, the reduction of cyanide ion concentration within the solution may be due to hydrocyanic acid evaporation [27].



As activated carbon is a granular adsorbent, the surface area of the internal pores is much larger than the external surface, so the copper or cobalt ferrites impregnated on the surface increases the oxidative capacity against cyanide by combining the carbon loading capacity, oxidation by activated carbon, and oxidation by the Mars van Krevelen mechanism. Therefore, cyanide can be treated by the three mentioned mechanisms, which can occur during the experimentation simultaneously. It can be asserted that the synthesized composites are suitable for the conversion of cyanide to cyanate reaching high percentages of oxidation.

In Figure 5, a difference in cyanide oxidation may be appreciated when the copper/cobalt activated carbon composites were calcined. In the case of CuFe-AC1000, which was the best composite for cyanide oxidation, a 90% oxidation of the cyanide ion was reached without further calcination treatment. On the other hand, the same composite with calcination reached 98% of the cyanide oxidation. However, it can be noted that the increase is only 8% without the calcination composite, despite the impregnation percentage of the ferrite increasing from 0.26% to 4.32%. Copper ferrites synthesized from the chemical precipitation method have a particle size smaller than 20 nm [12,28], which favors their sintering and agglomeration on the active carbon surface, so although there is more copper ferrite on the calcined composite, the active sites are scarce due to the aforementioned phenomena.

Regarding cobalt ferrites, it can be additionally observed that the calcined composite delivered a higher oxidation than without the CoFe-AC1000 composite. The difference in the degree of cyanide oxidation can be explained due to the calcination temperature, since it is possible that the structure of the spinel may be better formed by combining the cobalt and iron oxides and forming stable bonds of cobalt ferrite, without damaging the active sites of the carbon surface. Calcination treatment benefits are also evidenced in cobalt and iron dissolution during cyanide oxidation essays (see Figure S2). Therefore, it can be deduced that calcination permits ferrite formation and deposition on the support

diminishing their dissolution due to their refractoriness. The percentage of impregnation of Cobalt ferrite was also improved significantly from 0.28% to 7.47%, which increased cyanide oxidation from 87% to 98%.

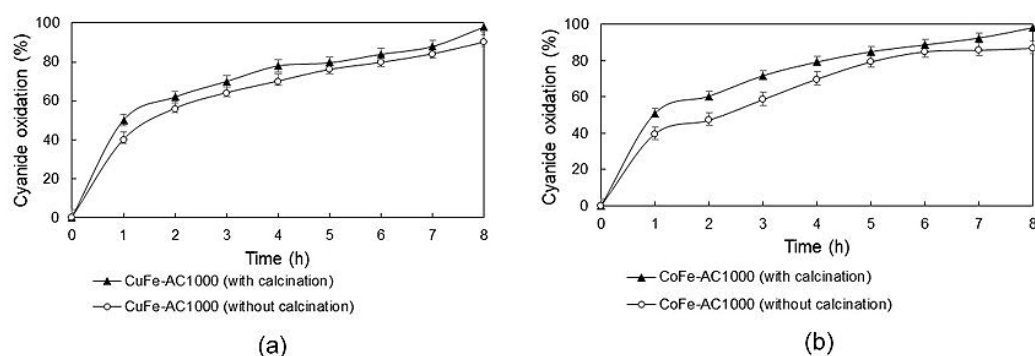


Figure 5. Cyanide oxidation: (a) CuF-AC1000 with and without calcination and (b) CoF-AC1000 with and without calcination. (Air flow = 180 NL/h; composite: solution ratio = 15 g/L.)

Lifespan tests were carried out using the CuFe-AC1000 and Co-AC1000 composites with calcination, since they presented the best results for cyanide ion oxidation. In the case of copper ferrite/activated carbon composite, cyanide oxidation diminished to 90% after the first recycle. In recycles 2, 3, and 4, the composite reached 80% of cyanide ion oxidation, while the fifth and last recycle reached a 70% oxidation. The decrease in the catalytic activity can be linked to the dilution of the copper ferrite in the sodium cyanide solution. During the recycles, copper, and iron concentration were measured using atomic absorption spectroscopy. The loss of these metals, which conforms to the spinels, decreased CuFe-AC1000 performance after several cyanide oxidation cycles.

In the case of cobalt ferrites, the lifespan of the CoFe-AC1000 composite with calcination was assessed as well, since it presented the best results in cyanide oxidation essays. After the first recycle, the catalytic activity of the composite diminished to 90%, as in the case of CuFe-AC1000. Nevertheless, after five recycles, cyanide ion oxidation never decreased from 80%, when CoFe-AC1000 composite was employed. Getting lost in the catalytic activity is possible, due to the wear suffered by the composite during the oxidation tests and the dissolution of cobalt and iron into the cyanide solution. Afterward, all oxidation essays were performed with stirring, the composites may break down by attrition. Thus, cobalt ferrites could be lost during the tests and the composite performance diminished, as it was demonstrated in Figure 6b.

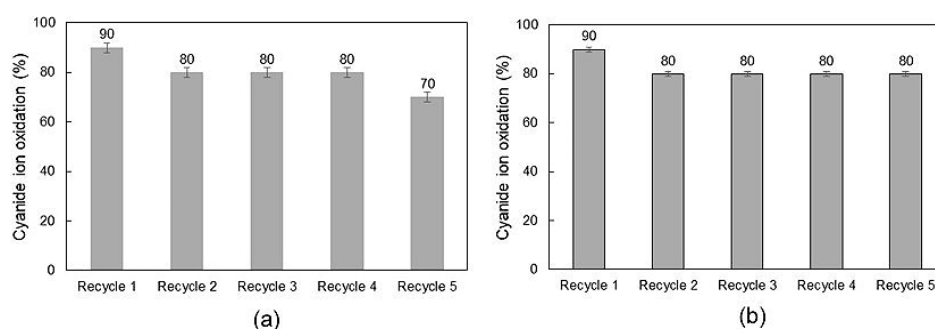


Figure 6. Oxidation percentage after 8 h for (a) CuFe-AC1000 and (b) CoFe-AC1000 composites.

The dissolution of the synthesized catalyst was measured during cyanide oxidation essays. In Table 4, the dissolution percentage of copper, cobalt, and iron dissolution is reported. Both copper and cobalt ferrites had low dissolution while they were in bulk. For CuFe₂O₄, the dissolution percentage for copper was 1.78%, whereas iron was 0.74%. For CoFe₂O₄, the dissolution percentage for cobalt was 0.04% and iron was 0.22%. For the supported catalyst, the dissolution of copper, cobalt,

and iron had higher results than bulk ferrites. For CuFe-AC1000, the dissolution of copper decreased while iron dissolution increased. On the other hand, for CoFe-AC1000, both cobalt and iron dissolution behaved in the same pattern. This different behavior can be attributed to the ferrite structure; spinel structure was achieved for cobalt ferrite, but for CuFe-AC1000, a copper-iron oxides system was formed in certain degree (See Figure 1). Copper and cobalt oxides (and not ferrites), synthesized during bulk ferrites formation using the co-precipitation method, may dissolve during cyanide oxidation essays, due to composites attrition, caused by 8 h of agitation. Cyanide ions may react with copper and cobalt oxides in order to form copper and cobalt cyanide complexes. These complexes of heavy metals may be removed from water bodies by employing adsorbents like zeolites, metal organic frameworks (MOFs), or activated carbon. It is well known that activated carbon has a high affinity for these complexes (especially for gold, silver, and copper cyanide complexes [27]). Nevertheless, other option could be the modification of these supports with polymers, like polydopamine, which have functional groups (amine groups) that may interact with copper and cobalt cyanide anionic complexes for their adsorption [29].

Table 4. Dissolution percentages for copper, cobalt, and iron.

Recycle	%Cu	%Fe	Recycle	%Co	%Fe
CuFe	1.78 ± 0.01	0.74 ± 0.01	CoFe	0.04 ± 0.01	0.22 ± 0.02
CuF-AC280	4.18 ± 0.02	0.43 ± 0.02	CoF-AC280	0.11 ± 0.02	0.12 ± 0.01
CuF-AC1000	5.27 ± 0.01	0.17 ± 0.01	CoF-AC1000	1.25 ± 0.01	1.62 ± 0.04
Recycle 1	4.64 ± 0.02	0.45 ± 0.02	Recycle 1	0.19 ± 0.02	0.30 ± 0.01
Recycle 2	4.38 ± 0.02	0.51 ± 0.01	Recycle 2	0.38 ± 0.01	0.35 ± 0.01
Recycle 3	3.10 ± 0.03	0.79 ± 0.01	Recycle 3	0.58 ± 0.02	0.81 ± 0.02
Recycle 4	2.85 ± 0.02	0.79 ± 0.01	Recycle 4	0.29 ± 0.02	0.61 ± 0.01
Recycle 5	2.46 ± 0.01	1.25 ± 0.01	Recycle 5	0.19 ± 0.01	0.35 ± 0.01

4. Conclusions

Copper ferrite and cobalt ferrite impregnated on activated carbon were successfully synthesized using the precipitation method. XRD and SEM techniques confirmed the formation of these ferrites and their deposition on activated carbon surface. The best composites resulted be the calcined CuFe-AC1000 and CoFe-AC1000 composites, which allowed to achieve a 98% cyanide ion oxidation after 8 h of agitation.

The calcination of copper/cobalt ferrite-activated carbon composites significantly improved the percentage of impregnation. This treatment permitted to form the spinel structure on activated carbon surface, which in turn allowed for the obtainment of better cyanide oxidation results, especially when compared to non-calcined composites. Therefore, calcination is an essential stage for copper/cobalt ferrite-activated carbon composite formations with the precipitation method. In addition, this treatment improved also improved composite performance during cyanide ion oxidation essays.

The useful life of the composites with greater catalytic activity were evaluated. There was a decrease in the oxidative capacity of 28% after five recycles in the CuFe-AC1000 composite and 18% in the CoFe-AC1000 composite. This decrease can be attributed to the attrition and loss of activated carbon in the tests and to the dissolution of copper, cobalt, and iron from the spinel.

In the case of copper ferrites-activated carbon composites, a higher percentage of iron dissolution was obtained compared to cobalt; however, the dissolution percentages did not exceed 2% Co, so it can be inferred that spinels exhibit high refractoriness in cyanide solutions. As for copper ferrites-activated carbon composites, greater copper dissolution than iron was detected in all essays. It is possible that copper oxides were still with the support, but were ultimately dissolved by cyanide ions. In the case of cobalt ferrites-activated carbon composites, cobalt dissolution did not exceed 1%, which confirms that cobalt losses were low. Therefore, the decrease in the concentration of cyanide was due to the oxidation of this reagent and not to the formation of copper and cobalt complexes with cyanide during all oxidation essays.

Supplementary Materials: The following are available online at <http://www.mdpi.com/2075-4701/8/12/1070/s1>, Figure S1: SEM images of CoFe₂O₄/AC1000 composite calcined by secondary electrons detector (SE) a 235x. (a) Before the acid wash. (b) After acid wash, Figure S2: Accumulated dissolution of copper and cobalt in the cyanide solution in 5 oxidation essays.

Author Contributions: Conceptualization, E.T.; Data curation, S.G.; Formal analysis, S.G.; Investigation, A.L. and M.A.; Methodology, A.L. and M.A.; Project administration, E.T.; Writing: original draft, S.G.; Writing: review and editing, S.G.

Funding: This research was funded by the Project PII-DEMEX-01-2017 of the Escuela Politécnica Nacional, which was executed in the Department of Extractive Metallurgy.

Acknowledgments: The authors address their thanks to the Escuela Politécnica Nacional for the support in the development of the present research.

Conflicts of Interest: The authors declare no conflict of interest. The funders had no role in the design of the study; in the collection, analyses, or interpretation of data; in the writing of the manuscript, or in the decision to publish the results.

References

1. Sarla, M.; Pandit, M.; Tyagi, D.K.; Kapoor, J.C. Oxidation of cyanide in aqueous solution by chemical and photochemical process. *J. Hazard. Mater.* **2004**, *116*, 49–56. [[CrossRef](#)] [[PubMed](#)]
2. Christoskova, S.; Stoyanova, M. Catalytic oxidation of cyanides in an aqueous phase over individual and manganese-modified cobalt oxide systems. *J. Hazard. Mater.* **2009**, *165*, 690–695. [[CrossRef](#)] [[PubMed](#)]
3. Pesántez, D.; de la Torre, E.; Guevara, A. Influencia del ion cúprico y del cobre metálico en la oxidación del cianuro libre con aire y carbón activo. Bachelor Thesis, Escuela Politecnica Nacional, Quito, Ecuador, 2008.
4. Knözinger, H.; Kochloefl, K. Heterogeneous Catalysis and Solid Catalysts. In *Ullmann's Encyclopedia of Industrial Chemistry*; Wiley VCH: Weinheim, Germany, 2003; pp. 2–110. ISBN 9783527306732.
5. Thomas, J.M. The societal significance of catalysis and the growing practical importance of single-site heterogeneous catalysts. *Proc. R. Soc. A Math. Phys. Eng. Sci.* **2012**, *468*, 1884–1903. [[CrossRef](#)]
6. Kharisov, B.I.; Dias, H.V.R.; Kharissova, O.V. Mini-review: Ferrite nanoparticles in the catalysis. *Arabian J. Chem.* **2014**, in press. [[CrossRef](#)]
7. Manova, E.; Tsoncheva, T.; Paneva, D.; Mitov, I.; Tenchev, K.; Petrov, L. Mechanochemically synthesized nano-dimensional iron-cobalt spinel oxides as catalysts for methanol decomposition. *Appl. Catal. A Gen.* **2004**, *277*, 119–127. [[CrossRef](#)]
8. Pourgolmohammad, B.; Masoudoanash, S.; Aboutalebi, A. Synthesis of CoFe₂O₄ powders with high surface area by solution combustion method: Effect of fuel content and cobalt precursor. *Ceram. Int.* **2017**, *43*, 3797–3803. [[CrossRef](#)]
9. Rashad, M.M.; Mohamed, R.M.; Ibrahim, M.A.; Ismail, L.F.M.; Abdel-Aal, E.A. Magnetic and catalytic properties of cubic copper ferrite nanopowders synthesized from secondary resources. *Adv. Powder Technol.* **2012**, *23*, 315–323. [[CrossRef](#)]
10. Tang, X.X.; Manthiram, A.; Goodenough, J.B. Copper ferrite revisited. *J. Solid State Chem.* **1989**, *79*, 250–262. [[CrossRef](#)]
11. Christoskova, S.G.; Stoyanova, M.; Georgieva, M. Low-temperature iron-modified cobalt oxide system Part 2. Catalytic oxidation of phenol in aqueous phase. *App. Catal. A Gen.* **2001**, *208*, 243–249. [[CrossRef](#)]
12. Manova, E.; Tsoncheva, T.; Paneva, D.; Popova, M.; Velinov, N.; Kunev, B.; Tenchev, K.; Mitov, I. Nanosized copper ferrite materials: Mechanochemical synthesis and characterization. *J. Solid State Chem.* **2011**, *184*, 1153–1158. [[CrossRef](#)]
13. Hirabayashi, D.; Yoshikawa, T.; Kawamoto, Y.; Mochizuki, K.; Suzuki, K. Characterization and Applications of Calcium Ferrites Based Materials Containing Active Oxygen Species. *Adv. Sci. Technol.* **2006**, *45*, 2169–2175. [[CrossRef](#)]
14. Kung, H.H.; Kung, M.C. Selective Oxidative Dehydrogenation of Butenes on Ferrite Catalysts. *Adv. Catal.* **1985**, *33*, 159–198. [[CrossRef](#)]
15. Stoyanova, M.; Christoskova, S.; Georgieva, M. Aqueous phase catalytic oxidation of cyanides over iron-modified cobalt oxide system. *Appl. Catal. A Gen.* **2004**, *274*, 133–138. [[CrossRef](#)]
16. Stoyanova, M.K.; Christoskova, S.G. Novel Ni-Fe- oxide systems for catalytic oxidation of cyanide in an aqueous phase. *Cent. Eur. J. Chem.* **2005**, *3*, 295–310. [[CrossRef](#)]

17. Rojas, N.; Bustamante, O. Copper dissolution from cupric ferrite in conventional cyanidation. Bachelor Thesis, Universidad Nacional de Colombia, Medellin, Colombia, May 2007; pp. 151–157. Available online: http://www.scielo.org.co/scielo.php?script=sci_arttext&pid=S0012-73532007000200013 (accessed on 17 July 2018).
18. Alexopoulou, C.; Petala, A.; Frontistis, Z.; Drivas, C.; Kennou, S.; Kondarides, D.I.; Mantzavinos, D. Copper phosphide and persulfate salt: A novel catalytic system for the degradation of aqueous phase micro-contaminants. *Appl. Catal. B Environ.* **2018**, *244*, 178–187. [[CrossRef](#)]
19. Musmarra, D.; Prisciandaro, M.; Capocelli, M.; Karatza, D.; Iovino, P.; Canzano, S.; Lancia, A. Degradation of ibuprofen by hydrodynamic cavitation: Reaction pathways and effect of operational parameters. *Ultrason. Sonochem.* **2016**, *29*, 76–83. [[CrossRef](#)] [[PubMed](#)]
20. Joshi, S.M.; Gogate, P.R. Treatment of landfill leachate using different configurations of ultrasonic reactors combined with advanced oxidation processes. *Sep. Purif. Technol.* **2019**, *211*, 10–18. [[CrossRef](#)]
21. Efome, J.E.; Rana, D.; Matsuura, T.; Lan, C.Q. Metal-organic frameworks supported on nanofibers to remove heavy metals. *J. Mater. Chem. A* **2018**, *6*, 4550–4555. [[CrossRef](#)]
22. Efome, J.E.; Rana, D.; Matsuura, T.; Lan, C.Q. Insight studies on metal-organic framework nanofibrous membrane adsorption and activation for heavy metal ion removal from aqueous solution. *ACS Appl. Mater. Interfaces* **2018**, *10*, 18619–18629. [[CrossRef](#)]
23. Efome, J.E.; Rana, D.; Matsuura, T.; Lan, C.Q. Experiment and modeling for flux and permeate concentration of heavy metal ions in adsorptive membrane filtration using a metal-organic framework incorporated nano-fibrous membrane. *Chem. Eng. J.* **2018**, *352*, 737–744. [[CrossRef](#)]
24. Kameoka, S.; Tanabe, T.; Tsai, A.P. Spinel CuFe₂O₄: A precursor for copper catalyst with high thermal stability and activity. *Catal. Lett.* **2005**, *100*, 89–93. [[CrossRef](#)]
25. De la Torre Chauvin, E. Préparation de charbon actif à partir de coques de noix de palmier à huile pour la récupération d'or et le traitement d'effluents cyanurés. Ph.D. Thesis, Université Catholique de Louvain, Louvain-La-Neuve, Belgium, 2015.
26. Pilco, Y. Estudio de la Oxidación de Efluentes Cianurados en Presencia de Aire y Carbón Activado. Bachelor Thesis, Escuela Politécnica Nacional, Quito, Ecuador, 2008.
27. De la Torre, E.; Gámez, S.; Pazmiño, E. Improvements to the cyanidation process for precious metal recovery from WPCBs. In *Waste Electrical and Electronic Equipment Recycling Aqueous Recovery Methods*; Biorloaga, I., Vegliò, F., Eds.; Woodhead Publishing Series in Electronic and Optical Materials: Duxford, UK, 2018; pp. 115–137. [[CrossRef](#)]
28. Ahamad, H.S.; Anand, K.; Meshram, N.S.; Rewatkar, G.K.; Dhoble, S.J. Synthesis and Characterization of Nanostructure Copper Ferrites by Microwave Assisted Sol-Gel Auto-Combustion Method. *Int. J. Lumin. Appl.* **2016**, *6*, 135–138.
29. Ball, V.; Del Frari, D.; Toniazzo, V.; Ruch, D. Kinetics of polydopamine film deposition as a function of pH and dopamine concentration: Insights in the polydopamine deposition mechanism. *J. Colloid Interface Sci.* **2012**, *386*, 366–372. [[CrossRef](#)] [[PubMed](#)]

